PHYSICAL REVIEW B **88**, 100406(R) (2013)

Large spin pumping from epitaxial $Y_3Fe_5O_{12}$ thin films to Pt and W layers

H. L. Wang,* C. H. Du,* Y. Pu, R. Adur, P. C. Hammel,† and F. Y. Yang‡
Department of Physics, The Ohio State University, Columbus, Ohio 43210, USA
(Received 1 July 2013; revised manuscript received 4 September 2013; published 18 September 2013)

Epitaxial $Y_3Fe_5O_{12}$ thin films deposited by off-axis sputtering exhibit excellent crystalline quality enabling observation of large spin pumping signals in Pt/$Y_3Fe_5O_{12}$ and W/$Y_3Fe_5O_{12}$ bilayers driven by cavity ferromagnetic resonance. The inverse spin Hall voltages reach 2.10 and -5.26 mV in 5-mm-long Pt/$Y_3Fe_5O_{12}$ and W/$Y_3Fe_5O_{12}$ bilayers, respectively, excited by a radio-frequency magnetic field of 0.3 Oe. From the ferromagnetic resonance linewidth broadening, we obtain high interfacial spin mixing conductances of 4.56×10^{14} and 2.30×10^{14} $\Omega^{-1}\,m^{-2}$ for Pt/$Y_3Fe_5O_{12}$ and W/$Y_3Fe_5O_{12}$ bilayers, respectively.

DOI: 10.1103/PhysRevB.88.100406 PACS number(s): 76.50.+g, 61.05.cp, 75.47.Lx, 75.70.Ak

Ferromagnetic resonance (FMR) driven spin pumping of pure spin currents has generated intense interest for its potential application in next-generation spintronics.[1–17] Due to the exceptionally low magnetic damping, insulating $Y_3Fe_5O_{12}$ (YIG) is potentially one of the best ferromagnets (FM) for microwave applications and FMR spin pumping.[1–9] The inverse spin Hall effect (ISHE) is an effective tool for studying spin pumping from FMs into nonmagnetic materials (NM).[1–4,12,14,15] In addition to Pt which is widely used as a NM due to its large ISHE, β-phase W and Ta are expected to generate large ISHE voltages (though of the opposite sign), making them attractive in this role as well. To date, no clear ISHE detection of FMR spin pumping in W/FM structures has been reported. Generating a high spin current density with a modest radio-frequency (rf) field, h_{rf}, requires a FM with low damping and YIG is highly attractive for this purpose.[18] In this Rapid Communication, we report observation of ISHE voltages, V_{ISHE}, of 2.10 (0.420 mV/mm) and 5.26 mV (1.05 mV/mm) for Pt/YIG and W/YIG bilayers, respectively, excited by a rf field of 0.3 Oe in a FMR cavity at the maximum rf power $P_{rf} = 200$ mW of our instrument.

The effectiveness of spin pumping depends on the degree to which the FM magnetization is excited by FMR, which in turn depends on the strength of the microwave fields h_{rf} used. Microwave cavities produce modest-strength rf fields that are uniform over a relatively large volume (centimeter scale), while rf fields from microstrip waveguides[3,7,8,12,19] are typically confined to micron or submillimeter volumes, but can generate fairly large h_{rf}.[12,19] Since reports on microstrip driven spin pumping often do not specify h_{rf},[12,19] we will compare our results with previous reports of spin pumping using cavity FMR.

Most YIG epitaxial films and single crystals are produced by liquid-phase epitaxy (LPE) with thicknesses from 100 nm to millimeters.[20] Pulsed laser deposition has been used to grow epitaxial YIG thin films,[21–23] but no ISHE measurements of spin pumping have been reported. Using our new ultrahigh vacuum, off-axis sputtering approach,[24–26] we deposit epitaxial YIG thin films on (111)-oriented $Gd_3Ga_5O_{12}$ (GGG) substrates.[27]

We determine the crystalline quality of the YIG films by high-resolution x-ray diffraction (XRD). A representative θ-2θ scan of a 20-nm YIG film shown in Fig. 1(a) indicates a phase-pure epitaxial YIG film. Figure 1(b) shows θ-2θ scans near the YIG (444) peak for four films with thicknesses $t =$ 10, 20, 50, and 80 nm, from which the out-of-plane lattice constant of the YIG films are obtained: $c = 12.426$, 12.393, 12.383, and 12.373 Å, respectively. Except for the 10-nm film, all other YIG films have lattice constants very close (within 0.14%) to the bulk value of 12.376 Å, indicating essentially strain-free films. Pronounced Laue oscillations are observed in all films, reflecting smooth surfaces and sharp YIG/GGG interfaces. The XRD rocking curves [insets to Fig. 1(b)] exhibit a FWHM of 0.027°, 0.0092°, 0.0072°, and 0.0053° for the 10-, 20-, 50-, and 80-nm-thick films, respectively, which reach the resolution limit of conventional high-resolution XRD systems, demonstrating excellent crystalline quality. In this Rapid Communication, we focus on two 20-nm YIG films (YIG-1 and YIG-2) for FMR and spin pumping measurements.

We perform room-temperature FMR measurements on the YIG films in a cavity at a microwave frequency $f = 9.65$ GHz and power $P_{rf} = 0.2$ mW. Figure 2 shows an FMR derivative spectrum of a 20-nm YIG film (YIG-1) with an in-plane magnetic field $\boldsymbol{H}$ along the x axis ($\theta_H = 90°$; see top-right inset to Fig. 2 for FMR measurement geometry), which gives a peak-to-peak linewidth (ΔH) of 7.42 ± 0.04 Oe obtained from a fit assuming a Lorentzian absorption line shape (for YIG-2, $\Delta H = 11.71 \pm 0.06$ Oe). The angular dependence of the resonance field (H_{res}) of the YIG film is shown in the bottom-left inset to Fig. 2(b), where H_{res} is defined as the field at which the derivative of the FMR absorption crosses zero. We obtain the effective magnetization $4\pi M_{eff} = 1794 \pm 36$ Oe from a numerical iterative analysis[27–29] of $H_{res}(\theta_H)$ that provides quantitative values in good agreement with those reported for single crystal YIG.[30]

Our spin pumping measurements are conducted at room temperature on three bilayer samples: Pt(5 nm)/YIG-1, Pt(5 nm)/YIG-2, and β-W(5 nm)/YIG-2, all made by off-axis sputtering. The approximately 1 mm × 5 mm samples are placed in the center of the FMR cavity with $\boldsymbol{H}$ applied in the xz plane, while the ISHE voltage is measured across a 5-mm-long Pt or W layer along the y axis, as illustrated in Fig. 3(a). The transfer of angular momentum to the Pt or W conduction electrons[31,32] resulting from FMR excitation of the YIG magnetization ($\boldsymbol{M}$) can be described as a spin current $\boldsymbol{J}_s$

 ©2013 American Physical Society

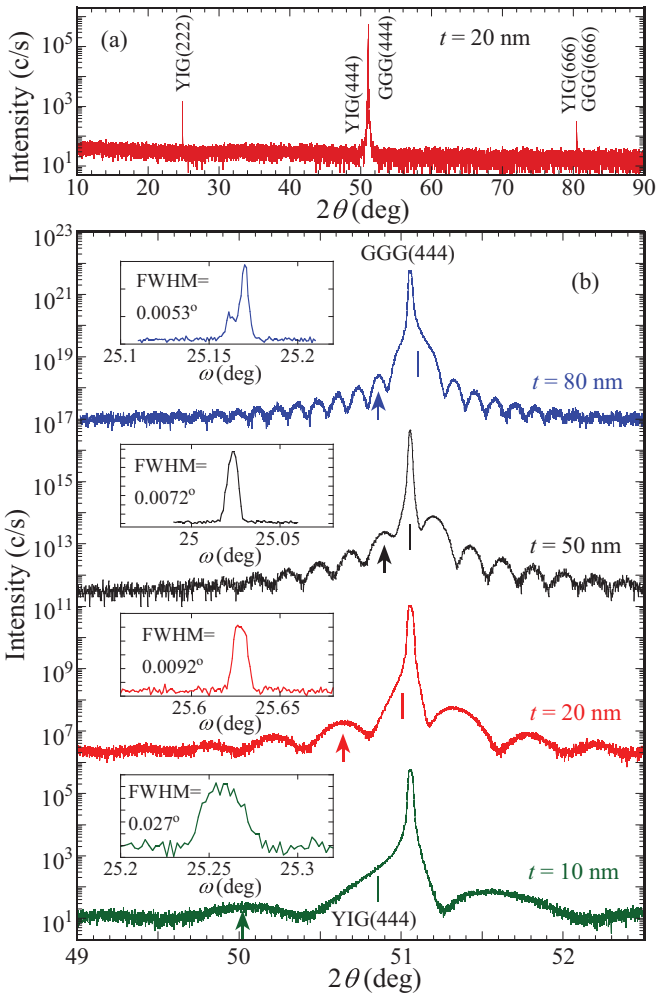

FIG. 1. (Color online) (a) Wide angle semilogarithmic θ-2θ XRD scan of a 20-nm-thick YIG film grown on GGG (111). (b) Semilogarithmic θ-2θ scans of 10-, 20-, 50-, and 80-nm-thick YIG films near the YIG (444) peak, all of which exhibit clear Laue oscillations corresponding to the film thickness. The vertical short lines mark the positions of the YIG (444) peak. The scans are offset from each other for clarity. The insets are the rocking curves of the four YIG films taken for the first satellite peak to the left of the man peak at the 2θ angle marked by the up arrows. The shoulder in the rocking curve of the 80-nm film is likely due to twinning in the film.

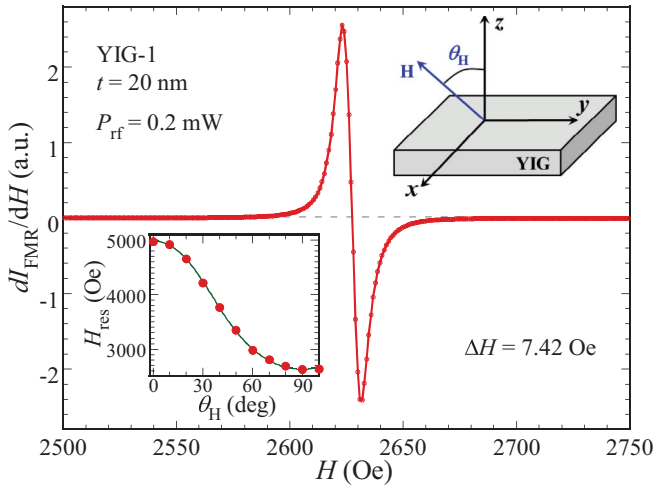

FIG. 2. (Color online) Room-temperature FMR derivative spectrum $dI_{\rm FMR}/dH$ vs H of a 20-nm YIG film (YIG-1) at $\theta_{\rm H} = 90^\circ$ (field in-plane) gives a linewidth of 7.42 Oe. Top-right inset: FMR experimental geometry. Bottom-left inset: fit (solid green curve) to the experimental data for the angular dependence of $H_{\rm res}$ for the YIG film from which we obtain $4\pi M_{\rm eff} = 1794$ Oe and $g = 2.0$.

injected along the z axis with its polarization (σ) parallel to $\boldsymbol{M}$. This spin current is converted by spin-orbit interactions to a charge current $\boldsymbol{J_c} \propto \theta_{\rm SH} \boldsymbol{J_s} \times \boldsymbol{\sigma}$, where $\theta_{\rm SH}$ is the spin Hall angle of Pt or W.[33] Figure 3(b) shows $V_{\rm ISHE}$ vs H spectra for Pt/YIG-1 and W/YIG-2 at $\theta_{\rm H} = 90^\circ$ (field in-plane) and $P_{\rm rf} = 200$ mW, which generates an rf field $h_{\rm rf} \sim 0.3$ Oe. At this moderate $h_{\rm rf}$ excitation, $V_{\rm ISHE}$ is quite large: 1.74 mV (0.35 mV/mm) in Pt/YIG-1 and 2.10 mV (0.42 mV/mm) in Pt/YIG-2, significantly larger than previously reported spin pumping signals using cavity FMR.[1,9–11,13–16] To account for the variation in FMR instrument parameters we compare FMR spin pumping results by normalizing to $h_{\rm rf}$ since $V_{\rm ISHE} \propto (h_{\rm rf})^2$. For example, $V_{\rm ISHE}$ of ~ 4.5 μV is reported in Pt/YIG at $P_{\rm rf} = 1$ mW with a nonlinear power dependence,[1] 340 μV in Pt/$BiY_2Fe_5O_{12}$ at $P_{\rm rf} = 200$ mW and $h_{\rm rf} = 1.6$ Oe,[9] and up to 70 μV in a series of Pt/FM systems at $h_{\rm rf} = 1.2$ Oe.[14] The noise voltage for the $V_{\rm ISHE}$ measurements is about 200 nV, so the values of $V_{\rm ISHE}$ are presented without error bars. The W/YIG-2 bilayer exhibits an even larger $V_{\rm ISHE}$ of -5.26 mV (-1.05 mV/mm), where the negative voltage reflects the opposite relative signs of the spin Hall angles of W and Pt.[34]

Figure 3(c) shows the rf-power dependence of $V_{\rm ISHE}$ for Pt/YIG-1 and W/YIG-2 at $\theta_{\rm H} = 90^\circ$. The linear relationship between $V_{\rm ISHE}$ and $P_{\rm rf}$ indicates that the observed ISHE voltage is not near saturation and can potentially be further increased by larger $h_{\rm rf}$ since $V_{\rm ISHE} \propto (h_{\rm rf})^2$.[19] Figure 3(d) shows a series of $V_{\rm ISHE}$ vs H spectra for varying $\theta_{\rm H}$ at $P_{\rm rf} = 200$ mW for the two samples. $V_{\rm ISHE}$ vs H is antisymmetric about $H = 0$ as expected for FMR spin pumping since reversal of $\boldsymbol{H}$ switches $\boldsymbol{M}$ (hence σ) and, consequently, changes the sign of $\boldsymbol{J_c}$. When $\boldsymbol{H}$ is rotated from in-plane to out-of-plane, $V_{\rm ISHE}$ gradually vanishes. $\boldsymbol{M}$ essentially follows $\boldsymbol{H}$ at all angles since 2500 Oe $< H_{\rm res} <$ 5000 Oe, all larger than $4\pi M_{\rm eff} = 1794$ Oe of our YIG film. Figure 3(e) shows the angular dependence of $V_{\rm ISHE}$ for Pt/YIG-1 and W/YIG-2 normalized by the maximum magnitude of $V_{\rm ISHE}$ at $\theta_{\rm H} = 90^\circ$. The clear sinusoidal shape is characteristic of ISHE since[15]

$$V_{\rm ISHE} \propto \boldsymbol{J_c} \propto \theta_{\rm SH} \boldsymbol{J_s} \times \boldsymbol{\sigma} \propto \theta_{\rm SH} \boldsymbol{J_s} \times \boldsymbol{M} \propto \theta_{\rm SH} \boldsymbol{J_s} \times \boldsymbol{H} \propto \theta_{\rm SH} \sin\theta_{\rm H}, \quad (1)$$

thus confirming that the observed ISHE voltage arises from FMR spin pumping. The spin pumping signals we observe in insulating YIG cannot be explained by artifacts due to thermoelectric or magnetoelectric effects, such as anisotropic magnetoresistance or anomalous Hall effect.[13,16,33,35,36]

A direct consequence of the transfer of angular momentum from YIG to metal by the spin current is an additional damping

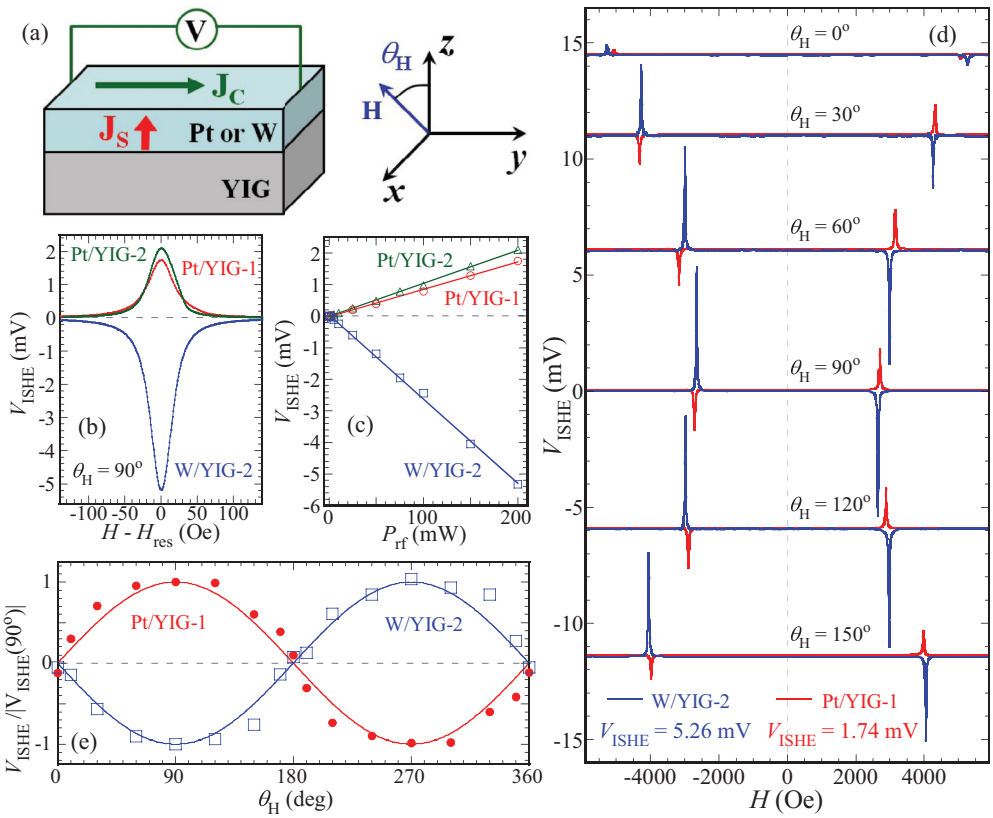

FIG. 3. (Color online) (a) Schematic diagram of the ISHE voltage measurement setup. (b) V_{ISHE} vs H spectra at $\theta_H = 90^\circ$ and $P_{rf} = 200$ mW for two Pt(5 nm)/YIG(20 nm) [Pt/YIG-1 and Pt/YIG-2] bilayers and a W(5 nm)/YIG(20 nm) [W/YIG-2] bilayer: ISHE voltages of 1.74, 2.10, and -5.26 mV, respectively, are observed. (c) Linear rf-power dependence of V_{ISHE} with a least-squares fit is shown for the three samples. (d) V_{ISHE} vs H spectra at different θ_H for Pt/YIG-1 and W/YIG-2. The curves are offset for clarity. The nonzero ISHE voltage at $\theta_H = 0^\circ$ and the difference in H_{res} between Pt/YIG-1 and W/YIG-2 at the same θ_H are due to slight misalignment of the sample with respect to $\boldsymbol{H}$. (e) Angular dependence of the normalized V_{ISHE} for Pt/YIG-1 and W/YIG-2, where the red and blue curves show $\sin\theta_H$ and $-\sin\theta_H$, respectively.

of the magnetization precession in YIG evident as an increase in linewidth,[10,12] as shown in Fig. 4 for the three samples before (ΔH_0) and after (ΔH_f) the deposition of Pt or W. A clear linewidth broadening is observed for all three samples: $\Delta H_f - \Delta H_0 = 19.91 \pm 0.10$, 24.34 ± 0.12, and 12.33 ± 0.06 Oe for Pt/YIG-1, Pt/YIG-2, and W/YIG-2, corresponding to V_{ISHE} values of 1.74, 2.10, and 5.26 mV, respectively (Table I). We note that the magnitude of V_{ISHE} appears to correlate more closely with the linewidth change than the original linewidth of the YIG films: Pt/YIG-2 has a larger linewidth increase (24.33 Oe) and V_{ISHE} (2.10 mV) than Pt/YIG-1 ($\Delta H_f - \Delta H_0 = 19.91$ Oe, $V_{ISHE} = 1.74$ mV) although YIG-2 ($\Delta H_0 = 11.71$ Oe) has a larger linewidth than YIG-1 ($\Delta H_0 = 7.42$ Oe). Though the original linewidth of a single YIG film determines the excited cone angle, this correspondence is expected since the spin current depends partially on the interfacial spin mixing conductance G which is proportional to the change in linewidth:[10,12]

$$G_r = \frac{e^2}{h}\frac{2\sqrt{3}\pi M_s \gamma t_F}{g\mu_B \omega}(\Delta H_f - \Delta H_0), \qquad (2)$$

where G_r, γ, g, and μ_B are the real part of spin mixing conductance, the gyromagnetic ratio, g factor, and Bohr magnetron, respectively. Using Eq. (2), we obtain $G_r = (4.56 \pm 0.16) \times 10^{14}$ and $(2.30 \pm 0.08) \times 10^{14}$ $\Omega^{-1}\,m^{-2}$ for Pt/YIG-2 and W/YIG-2, respectively, which agree with the theoretical calculations[37] and are among the highest of reported experimental values.[3,5,8,9]

ISHE voltages arising from spin pumping of Pt/YIG excited by similar cavity FMR typically gives voltages in the μV range.[1,9,11,16] The large spin pumping signals and high spin mixing conductances observed in our YIG films may have two origins. First, our films are very thin (20 nm) compared to LPE films (100 nm or larger); this may play an important role, as suggested by a recent report[7] that a 200-nm YIG film shows much higher spin pumping efficiency than 1- and 3-μm films excited by a microstrip waveguide. Second, our off-axis sputtered films may differ in crystalline quality or FMR characteristics from those made by other techniques. Compared to cavity FMR, microstrip waveguides can potentially provide much stronger rf fields, e.g., 16 Oe in Ref. 19 and 4.5 Oe in Ref. 12, and this can significantly increase the magnitude of ISHE voltages ($V_{ISHE} \propto h_{rf}^2$ in the linear regime).[7,12] We will study spin pumping in these thin YIG films using microstrip waveguides to access a larger dynamic range of spin pumping. In addition, the mV-level ISHE voltages reported

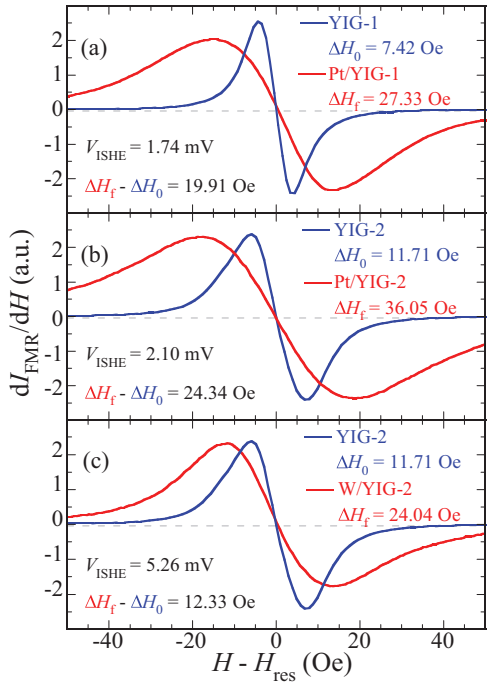

FIG. 4. (Color online) FMR derivative absorption spectra of YIG thin films at $P_{rf} = 0.2$ mW before (ΔH_0, blue) and after (ΔH_f, red) the deposition of (a) 5-nm Pt on YIG-1 ($V_{ISHE} = 1.74$ mV), (b) 5-nm Pt on YIG-2 ($V_{ISHE} = 2.10$ mV), and (c) 5-nm W on YIG-2 ($V_{ISHE} = 5.26$ mV), which show linewidth increases from $\Delta H_0 = 7.42$ Oe to $\Delta H_f = 27.33$ Oe, from 11.71 Oe to 36.05 Oe, and from 11.71 Oe to 24.04 Oe, respectively.

TABLE I. FMR linewidths of original YIG films, linewidth changes in metal/YIG bilayers, ISHE voltages at $P_{rf} = 200$ mW, and interfacial spin mixing conductances of the three bilayer samples.

Bilayers	ΔH_0 (Oe)	$\Delta H_f - \Delta H_0$ (Oe)	V_{ISHE} (mV)	G_r (Ω^{-1} m^{-2})
Pt/YIG-1	7.42	19.91	1.74	3.73×10^{14}
Pt/YIG-2	11.71	24.34	2.10	4.56×10^{14}
W/YIG-2	11.71	12.33	5.26	2.30×10^{14}

here using a moderate h_{rf} will allow miniaturization of spin pumping structures while maintaining signals sufficiently large to explore opportunities such as magnon-based electronics and other next-generation technologies.[18] It also provides a material platform for probing the fundamental mechanisms in spin pumping for quantitative characterization of coupling mechanisms and interfacial phenomena.

This work is supported by the Center for Emergent Materials at the Ohio State University, a NSF Materials Research Science and Engineering Center (Grant No. DMR-0820414) (H.L.W., Y.P., and F.Y.Y.), and by the Department of Energy through Grant No. DE-FG02-03ER46054 (R.A. and P.C.H.). Partial support is provided by Lake Shore Cryogenics Inc. (C.H.D.). The NanoSystems Laboratory at the Ohio State University provided technical support.

*These authors made equal contributions to this work.
†hammel@physics.osu.edu
‡fyyang@physics.osu.edu

[1] Y. Kajiwara, K. Harii, S. Takahashi, J. Ohe, K. Uchida, M. Mizuguchi, H. Umezawa, H. Kawai, K. Ando, K. Takanashi, S. Maekawa, and E. Saitoh, Nature (London) **464**, 262 (2010).
[2] C. W. Sandweg, Y. Kajiwara, A. V. Chumak, A. A. Serga, V. I. Vasyuchka, M. B. Jungfleisch, E. Saitoh, and B. Hillebrands, Phys. Rev. Lett. **106**, 216601 (2011).
[3] V. Castel, V. Vliestra, J. Ben Youssef, and B. J. van Wees, Appl. Phys. Lett. **101**, 132414 (2012).
[4] H. Kurebayashi, O. Dzyapko, V. E. Demidov, D. Fang, A. J. Ferguson, and S. O. Demokritov, Appl. Phys. Lett. **99**, 162502 (2011).
[5] B. Heinrich, C. Burrowes, E. Montoya, B. Kardasz, E. Girt, Y.-Y. Song, Y. Sun, and M. Wu, Phys. Rev. Lett. **107**, 066604 (2011).
[6] S. M. Rezende, R. L. Rodríguez-Suárez, M. M. Soares, L. H. Vilela-Leão, D. Ley Domínguez, and A. Azevedo, Appl. Phys. Lett. **102**, 012402 (2013).
[7] V. Castel, N. Vlietstra, J. Ben Youssef, and B. J. van Wees, arXiv:1304.2190.
[8] C. Hahn, G. de Loubens, O. Klein, M. Viret, V. V. Naletov, and J. Ben Youssef, Phys. Rev. B **87**, 174417 (2013).
[9] R. Takahashi, R. Iguchi, K. Ando, H. Nakayama, T. Yoshino, and E. Saitoh, J. Appl. Phys. **111**, 07C307 (2012).
[10] E. Shikoh, K. Ando, K. Kubo, E. Saitoh, T. Shinjo, and M. Shiraishi, Phys. Rev. Lett. **110**, 127201 (2013).
[11] A. Azevedo, L. H. Vilela Leão, R. L. Rodriguez-Suarez, A. B. Oliveira, and S. M. Rezende, J. Appl. Phys. **97**, 10C715 (2005).
[12] O. Mosendz, V. Vlaminck, J. E. Pearson, F. Y. Fradin, G. E. W. Bauer, S. D. Bader, and A. Hoffmann, Phys. Rev. B **82**, 214403 (2010).
[13] K. Ando, S. Takahashi, J. Iead, H. Kurebayashi, T. Trypiniotis, C. H. W. Barnes, S. Maekawa, and E. Saitoh, Nat. Mater. **10**, 655 (2011).
[14] F. D. Czeschka, L. Dreher, M. S. Brandt, M. Weiler, M. Althammer, I.-M. Imort, G. Reiss, A. Thomas, W. Schoch, W. Limmer, H. Huebl, R. Gross, and S. T. B. Goennenwein, Phys. Rev. Lett. **107**, 046601 (2011).
[15] K. Ando, Y. Kajiwara, S. Takahashi, S. Maekawa, K. Takemoto, M. Takatsu, and E. Saitoh, Phys. Rev. B **78**, 014413 (2008).
[16] K. Ando, S. Takahashi, J. Ieda, Y. Kajiwara, H. Nakayama, T. Yoshino, K. Harii, Y. Fujikawa, M. Matsuo, S. Maekawa, and E. Saitoh, J. Appl. Phys. **109**, 103913 (2011).
[17] J. Chow, R. J. Kopp, and P. R. Portney, Science **302**, 1528 (2003).
[18] A. A. Serga, A. V. Chumak, and B. Hillebrands, J. Phys. D: Appl. Phys. **43**, 264002 (2010).
[19] M. V. Costache, M. Sladkov, S. M. Watts, C. H. van der Wal, and B. J. van Wees, Phys. Rev. Lett. **97**, 216603 (2006).
[20] R. C. Linares, R. B. McGraw, and J. B. Schroeder, J. Appl. Phys. **36**, 2884 (1965).

[21]P. C. Dorsey, S. E. Bushnell, R. G. Seed, and C. Vittoria, J. Appl. Phys. **74**, 1242 (1993).

[22]S. A. Manuilov, R. Fors, S. I. Khartsev, and A. M. Grishin, J. Appl. Phys. **105**, 033917 (2009).

[23]Y. Sun, Y. Song, H. Chang, M. Kabatek, M. Jantz, W. Schneider, M. Wu, H. Schultheiss, and A. Hoffmann, Appl. Phys. Lett. **101**, 152405 (2012).

[24]A. J. Hauser, R. E. A. Williams, R. A. Ricciardo, A. Genc, M. Dixit, J. M. Lucy, P. M. Woodward, H. L. Fraser, and F. Yang, Phys. Rev. B **83**, 014407 (2011).

[25]A. J. Hauser, J. R. Soliz, M. Dixit, R. E. A. Williams, M. A. Susner, B. Peters, L. M. Mier, T. L. Gustafson, M. D. Sumption, H. L. Fraser, P. M. Woodward, and F. Y. Yang, Phys. Rev. B **85**, 161201(R) (2012).

[26]C. Du, R. Adur, H. Wang, A. J. Hauser, F. Yang, and P. C. Hammel, Phys. Rev. Lett. **110**, 147204 (2013).

[27]See Supplemental Material at http://link.aps.org/supplemental/10.1103/PhysRevB.88.100406 for details of film deposition and FMR analysis.

[28]M. Farley, Rep. Prog. Phys. **61**, 755 (1998).

[29]Y. Q. He and P. E. Wigen, J. Magn. Magn. Mater. **53**, 115 (1985).

[30]P. Hansen, P. Röschmann, and W. Tolksdorf, J. Appl. Phys. **45**, 2728 (1974).

[31]E. Saitoh, M. Ueda, H. Miyajima, and G. Tatara, Appl. Phys. Lett. **88**,182509 (2006).

[32]B. Heinrich, Y. Tserkovnyak, G. Woltersdorf, A. Brataas, R. Urban, and G. E. W. Bauer, Phys. Rev. Lett. **90**, 187601 (2003).

[33]L. Liu, C. F. Pai, Y. Li, H. W. Tseng, D. C. Ralph, and R. A. Buhrman, Science **336**, 555 (2012).

[34]C. F. Pai, L. Liu, Y. Li, H. W. Tseng, D. C. Ralph, and R. A. Buhrman, Appl. Phys. Lett. **101**, 122404 (2012).

[35]M. Harder, Z. X. Cao, Y. S. Gui, X. L. Fan, and C. M. Hu, Phys. Rev. B **84**, 054423 (2011).

[36]S. Y. Huang, X. Fan, D. Qu, Y. P. Chen, W. G. Wang, J. Wu, T. Y. Chen, J. Q. Xiao, and C. L. Chien, Phys. Rev. Lett. **109**, 107204 (2012).

[37]Y. T. Chen, S. Takahashi, H. Nakayama, M. Althammer, S. T. B. Goennenwein, E. Saitoh, and G. E. W. Bauer, Phys. Rev. B **87**, 144411 (2013).